Fullerenol Synthesis and Identification. Properties of the Fullerenol Water Solutions

Konstantin N. Semenov,*,† Nikolai A. Charykov,† and Viktor N. Keskinov‡

Saint-Petersburg State University, Universitetskii pr. 26, St. Petersburg, Russia 198504, and ILIP Ltd. (Innovations of Leningrad Universities and Enterprises), Instrumentalnaya ul. 6, St. Petersburg, Russia 197022

This paper describes the synthesis and identification of the fullerenol, and data on the temperature dependence of solubility in water, concentration dependence of density, hydrogen ion concentration, molar conductivity, dissociation constant, and dynamic light scattering are presented. The composition of equilibrium solid phase in the binary fullerenol + water system is determined.

Introduction

Light fullerenes (C_{60} and C_{70}) can be used in various areas of science and engineering, including materials science, mechanics, mechanical engineering, construction, electronics, optics, medicine, pharmacology, and the food and cosmetic industry.[1,2] However the application of light fullerenes is limited due to low solubility of fullerenes in water and aqueous solutions. For example, the solubility of C_{60} in water at 25 °C according to refs 2−6 is equal to 1.3×10^{-11} g·L^{-1}, and the solubility of C_{70} is equal to 1.1×10^{-13} g·L^{-1}.[3−8] Light fullerenes derivatives (fluoro, chloro, bromo, iodo, amino, carboxo, etc.) are also practically insoluble in water and aqueous solutions. However, they have been extensively used in mechanical engineering (in water-soluble freezing and antifriction compositions), construction (as a soluble additives to cements and concretes), medicine and pharmacology (due to compatibility with water, physiological solutions, lymph, blood, digestive juices etc.), and cosmetology (in the case of using of water and water + alcohol solutions).[6−9]

Particularly, water-soluble films surfaces based on fullerenols can be used in micro- and optoelectronics, due to the following reasons: they can be extremely thin films (the thickness of such surfaces varies from 10 nm up to 1 μm); they have a high adhesion to metal, alloys, and semiconductors (A^3B^5, A^2B^6, A^4B^4, et al. types) surfaces; their transparency in visible and infrared spectrum regions is high; light-absorption in near-by ultraviolet spectral region is strong; in the far light-spectrum region such films are opaque; the refraction index is low; the chemical and thermostability is high.

During the hydroxylation of fullerenes mixtures of various polyhydroxylated fullerenes can be obtained.[10] For example, hydroxylation of the C_{60} fullerene in the presence of quaternary ammonium bases results in $C_{60}(OH)_{26,5}$-derivative. In the case of using HNO_3/H_2SO_4−acids mixture, the $C_{60}(OH)_{18-20}$-derivative formation takes place.[11,12] By the hydrolysis of the products of the RuO_4 and fullerenes reaction the diols 1,2-$C_{60}(OH)_2$, 1,2-$C_{70}(OH)_2$, and 5,6-$C_{70}(OH)_2$ can be synthesized. Due to the instability of such derivatives, their application in biological experiments is impracticable.[13] The $C_{60}(OH)_{24}$ fullerenol can be obtained by the reaction of alkaline hydrolysis of the polybromosubstituted $C_{60}Br_{24}$ fullerene.[14,22] We conclude that the fullerenols obtained by the methods presented in the literature leads to products of different structures and can be characterized by poor reproducibility and makes difficulties for experimental studies. Moreover, it has been shown that the fullerenol obtained by the reaction of the C_{60} fullerene with tertrabutylammonium hydroxide (TBAH) in toluene in the presence of oxygen and water solution of NaOH, is a stable anion-radical $Na_n^+[C_{60}O_xOH_y]_n^-$ (where $n = 2-3$, $x = 7-9$, and $y = 12-15$).[15] Due to the low solubility of nonhydroxylated fullerenes, the rate of the direct reaction between C_{60} and hydrogen peroxide is rather slow, therefore it is more convenient to add the complementary hydroxy-groups to the hydroxylated fullerenol with 12 hydroxy-groups. The authors of ref 16 carried out the reaction between the fullerenol with 12 hydroxy-groups and H_2O_2 (1) + H_2O (2) with $\omega_1 = 0.13$ at 60 °C with shaking. Thus, the $C_{60}(OH)_{36}\cdot 8H_2O$ and $C_{60}(OH)_{40}\cdot 9H_2O$ fullerenols with different compositions and structures were synthesized over several days. Yang et al.[17] described the convenient and effective method of the fullerenol synthesis; polyethylene glycol 400 (PEG) as a catalyst was added to the reaction mixture containing fullerenes, aqueous solution of NaOH, and an oxidizing agent. Sheng et al.[18,19] synthesized fullerenols by the direct reaction between the fullerene dredge and H_2O_2 + NaOH mixture. The eleven methods for the water-soluble fullerenols synthesis ($C_{60}(OH)_1$, $C_{60}(OH)_6$, $C_{60}(OH)_8$, $C_{60}(OH)_{x<12}$, $C_{60}(OH)_{12}$, $C_{60}(OH)_{x>15}$, $C_{60x<5}(OH)_{15}$, $C_{60}(OH)_{x<21}$, $C_{60}(OH)_{24}$, et al.) were described in a U.S. patent.[19] The authors of refs 20 and 21 synthesized the highly water-soluble fullerenols by the direct oxidation reaction of the C_{60} fullerene under normal conditions. The fullerenols obtained retain the biological and chemical properties of the C_{60} fullerene; that allows using such derivatives in water-soluble oils, as additives to spirit production, in pharmacology, and in medicine.

Experimental Section

Fullerene C_{60} of mass fraction purity 99.9%, with the main detectable impurity C_{70} ($w = 0.001$) was used. The reagent was produced at ZAO "ILIP" (St. Petersburg). The other reagents used were reagent grade 10% tetrabutylammonium hydroxide (TBAH), benzene, methanol, and water were distilled, NaOH (purchased from Vecton Ltd., St.-Petersburg).

* Corresponding author. Tel.: (812)3476435. Fax: (812)2349859. E-mail: semenov1986@yandex.ru.
† Saint-Petersburg State University.
‡ ILIP Ltd.

10.1021/je100755v
Published on Web 01/10/2011

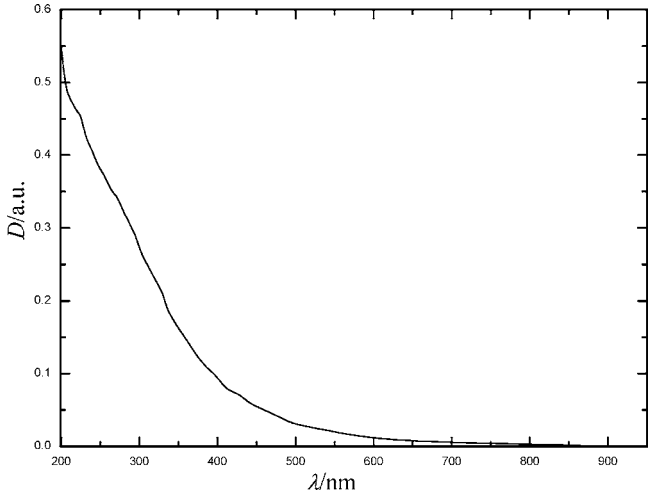

Figure 1. Optical spectrum of the fullerenol water solution. *D* is optical density; λ, wavelength.

Synthesis of the Fullerenol. The most simple and repeatable method of the direct fullerenol synthesis was chosen.[10,20] Initially a fullerene solution in benzene (600 mg of C_{60} and 800 mL of benzene) was prepared. The saturation of the solution was carried out in the temperature-controlled shaker at $t = (20 \pm 0.1)$ °C during 20 h. After that the solution was filtered with a Schott filter (porosity factor 10). Then the water solution of NaOH (20 g of NaOH in 20 mL of H_2O) and 20% tetrabutylammonium hydroxide solution (1.5 to 2) mL were added to the C_{60} solution in benzene up to decolouration of the benzene solution. After that, the benzene was distilled under vacuum (666.6 Pa) from the reaction mixture, and a supplementary quantity of distilled water (100 mL) was added. The reaction mixture obtained was stirred with a magnetic stirrer for (12 to 15) h, and during this process the extraction of the fullerenol to the water phase was realized. Then an additional quantity of water (200 mL) was added for the completion of the reaction. The mixture obtained was filtered on the Schott filter (porosity factor 10), and the solution was evaporated using the rotary evaporator up to 50 mL. After that 500 mL of methanol was added and the fullerenol was precipitated from the water solution in the form of brown flaky precipitate (the reprecipitation procedure was repeated 3 times). Then the precipitate was separated from the solution and additionally washed by methanol up to neutral value of pH = 7 ± 1 and dried in vacuum at $t =$ 40 °C and $p = 13.3$ Pa. As a result the reddish-brown fine crystals of the fullerenol were obtained; the yield of the reaction was equal to 72% (600 mg).

UV Spectrum of the Fullerenol. Visible and near UV electron spectra of the aqueous solution of the fullerenol related to pure water are presented in Figure 1. The spectra were obtained on a SPECORD M-32 spectral photometer in quartz cuvettes of 1 cm width within the wavelength range of (200 to 900) nm. Figure 1 shows that the spectrum does not contain a visible absorption zone. In particular, no absorption peaks typical for the light fullerenes and their derivatives in aromatic and nonaromatic solvents were observed near 472 nm (for the fullerene C_{70}), near 335 nm (for both fullerenes C_{60} and C_{70}) and (320 to 330) nm (for bromine-fullerenes $C_{60}Br_n$ ($n = 6$, 8, 24).[1,11−14,23,24] As a whole, the UV spectra of the fullerenol solutions turned out to be not informative enough but can be used for the composition determination. For example, the determination of the fullerenol composition is possible in aqueous environments if the wavelengths $\lambda = (300$ to 500) nm, where the absorption is not too high.

IR Spectrum of the Fullerenol. To identify the fullerenol, we analyzed its IR absorption spectra on a SHIMADZU FTIR-8400S spectrometer. Potassium bromide KBr tablets (dried in Ar) were used. The wavenumber range was $\tilde{\nu} = (400$ to 4400) cm^{-1}. The fullerenol IR spectrum showed a broad hydroxy absorption centered at 3420 cm^{-1}, a C-0 stretching absorption centered at 1040 cm^{-1} and a C═C absorption centered at about 1600 cm^{-1}. A spectrum of the solid fullerenol, known from literature agreed well with the obtained spectrum.[21] Some principal absorption peaks, e.g., the duplets at $\tilde{\nu}_2{}^1 \approx 1590$ cm^{-1}, $\tilde{\nu}_2{}^2 \approx 1450$ cm^{-1} remain invariable for both the fullerene C_{60} and the fullerenol. So, the fullerenol IR spectra can be effectively used for its identification.

Mass Spectrum of the Fullerenol. The mass-spectrum measurements were carried out on the MICROTOF mass-spectrometer (Bruker).

The mass-spectrometric peaks, concerning to *m*/*z* ratio equal to (970 to 1317) a.u. are clearly seen on the mass-spectrum. These peaks can be attributed to the total content of oxygen in $C_{60}(OH)_{n_1}O_{n_2}$ and $C_{60}(OH)_{n_1}O_{n_2}(ONa)_{n3}$ ($n_1 + n_2 + n_3 \approx 12$ to 34) molecules constituent the fullerenol. The average *m*/*z* ratio predicted for the fullerenol molecule $C_{60}(OH)_{22\div24}$ is equal to (1094 to 1128) a.u. For instance, the intensive mass-spectrometric peaks at $m/z \approx 969$ a.u. can be matched up with $C_{60}(OH)_{10}(ONa)_2$ ($m = 968$ a.u.) form. The next peak at $m/z \approx$ 985 a.u. ($z = 1$) corresponds to $C_{60}(OH)_{10}O_1(ONa)_2$, the peak at $m/z \approx 1013$ a.u. ($z = 1$) corresponds to $C_{60}(OH)_{15}(ONa)_1$ and so forth up to the $m/z \approx 1317$ a.u. value, the latest value corresponds to $C_{60}(OH)_{30}O_3(ONa)_1$. In all further calculations the relative molecular weight corresponded to the $C_{60}(OH)_{24}$ fullerenol formula equal to 1128 a.u. was accepted.

Determination of the Fullerenol Solubility in Water. By the isothermal saturation method in ampules we have investigated the solubility of the fullerenol in the distilled water in the temperature range (20 to 80) °C. The saturation conditions were the following: the time of saturation was equal to 120 min, the saturation of solutions was carried out in the temperature-controlled shaker (the saturation temperature was maintained with ± 0.05 °C uncertainty), the shaking frequency was equal to 80 s^{-1}, the analysis of the fullerenol concentration in the saturated solutions was determined by the gravimetric method, the mass change in the process of evaporation of water from the solution at (50 ± 2) °C and 13.3 Pa was calculated.

Equilibrium Solid Crystallohydrate Composition Determination. For determination of the equilibrium fullerenol crystallohydrate ($C_{60}(OH)_{22}{}^x \div nH_2O$) composition the saturation of the fullerenol water solution in the temperature-controlled shaker at (25 ± 0.05) °C for 4 h was performed. After that the solid phase was filtered and rapidly washed by methanol. The crystallohydrate obtained was weighed and dried in vacuum (13.3 Pa) at $t \approx (50 \pm 2)$ °C, and then weighed again. The relative mass change ($\Delta m_{\text{fullerenol-hydrate}}/m_{\text{fullerenol-hydrate}} \approx 0.30$) corresponded to the solvent content in the initial crystal solute. Thus the quantity of water molecules per one molecule of fullerenol is equal to 98 units. Thus the formula of the crystallohydrate is $C_{60}(OH)_{22\div24}\cdot 30H_2O$. Additionally the thermogravimetric thermal analysis of the fullerenol crystallohydrate was performed. The heating of the samples was carried in the open air with the heating rate equal to 5 K/min. According to the thermal analysis data the water content in the equilibrium crystallohydrate $C_{60}(OH)_{22\div24}\cdot nH_2O$ is equal to $n = 30 \pm 2$. The fullerenol crystallohydrate dissociation can be expressed by the two-stage scheme:

$$C_{60}(OH)_{22\div24}\cdot 30H_2O(solid) \rightarrow C_{60}(OH)_{22\div24}\cdot 15H_2O(solid) + 15H_2O(gas),\quad t_1^{diss} \approx (100 \pm 2)\ ^\circ C \quad (1.1)$$

$$C_{60}(OH)_{22\div24}\cdot 15H_2O(solid) \rightarrow C_{60}(OH)_{22\div24}(solid) + 15H_2O(gas),\quad t_2^{diss} \approx (119 \pm 2)\ ^\circ C \quad (1.2)$$

With increasing of temperature the expansion of the fullerenol hydroxyls takes place according to reaction

$$C_{60}(OH)_{22\div24}(solid) \rightarrow C_{60}O_{11\div12}(solid) + (11\ to\ 12)H_2O(gas),\quad t_3^{diss} \approx (852 \pm 5)\ ^\circ C \quad (1.3)$$

Fullerenol Water Solutions Densities Determination. The concentration dependence of density determination of the fullerenol water solutions at 25 °C was carried out by the picnometer method[29] using quartz picnometers. The volume calibration was performed using water, the uncertainty of thermostatting was $\Delta t = \pm 0.1$ K. The fullerenol water solutions were prepared by the direct dissolution of the fullerenol in the water. Then the heterogeneous mixture was stirred during 1 h at 25 °C and filtered. The mass concentration of the initial solution was determined by the gravimetric method. The other samples were prepared by the dilution of the basic solution. The fullerenol concentrations were calculated from the data on masses of fullerenol solutions and water.

Fullerenol Water Solutions Refractive Index Determination. The dependence between refractive index of the fullerenol water solutions d (n_D^{25}) and concentration was determined by the refractometry method on the IRF-454B2M refractometer (the uncertainty of the refractive index determination is equal to $\Delta n_D^{20} = \pm 0.0001$; the thermostatting uncertainty is equal to $\pm$ 0.05 °C).[31]

Determination of the Hydrogen Ion Concentration of the Fullerenol Water Solutions. Hydrogen ion concentration (pH) of the fullerenol water solution was carried out by the pH-potentiometry method using Delta 320 pH-meter and InLab 413 electrode (three-in-one). The uncertainty of the hydrogen ion concentration determination (ΔpH) equal to 0.05 arbitrary units. All measurements were carried out in air atmosphere at (22 ± 2) °C, and the solutions were saturated by atmosphere air, including carbon dioxide (CO_2).

Determination of the Specific Conductivity of the Fullerenol Water Solutions. For determination of the specific conductivity of the fullerenol water solutions the Cyber Scan PC-300 measuring device was used. The relative uncertainty of the specific conductivity determination is equal ± 1 %. The solutions used were saturated by atmospheric air.

Potentiometric Titration of the Fullerenole Water Solutions by NaOH and H_2SO_4. The potentiometric titration of the fullerenol water solutions was carried out at 25 °C using 0.004 mol·L^{-1} solution of H_2SO_4 and 1.0 mol·L^{-1} solution of NaOH. The titration was carried out using Delta 320 pH-meter and InLab 413 electrode (three-in-one). The accuracy (ΔpH) is equal to 0.05 arbitrary units. In the case of titration by H_2SO_4 solution the titrate contained $2.32 \cdot 10^{-5}$ mol of the fullerenol dissolved in 20 mL of water; the molarity of the fullerenol solution was equal to 0.00116 mol·L^{-1}. In the case of titration by NaOH solution, the titrate contained $2.04 \cdot 10^{-4}$ mol of the fullerenol dissolved in 20 mL of water; the molarity of the fullerenol solution was equal to 0.0204 mol·L^{-1}.

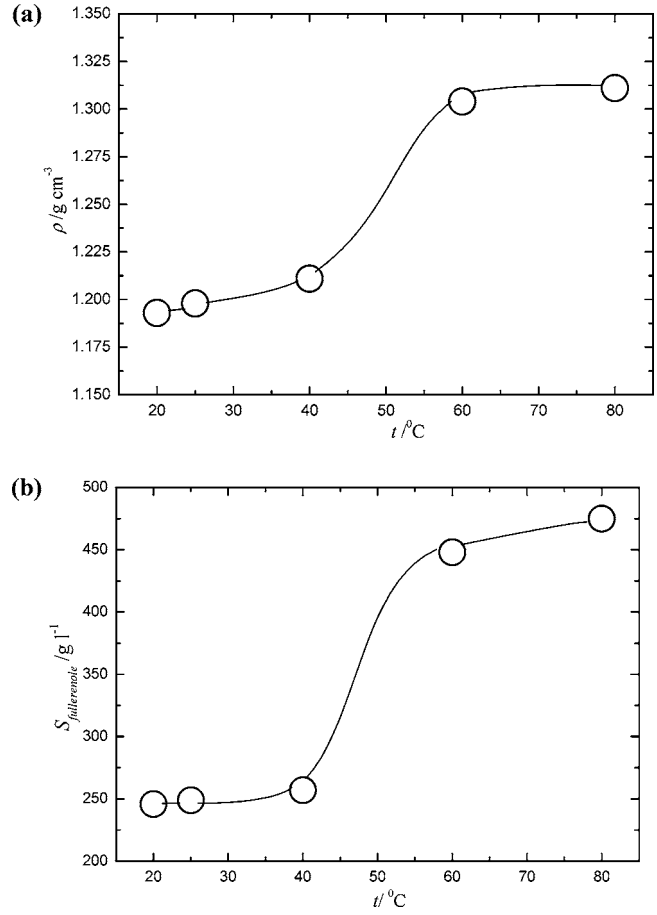

Figure 2. Temperature dependences of density of the fullerenol in water in the temperature range from (20 to 60) °C (a). Temperature dependence of the fullerenol solubility in water in the volume concentrations (b).

Fullerenol Nanoparticles Size Distribution in Aqueous Solutions. The Electrokinetic Potential Measurements. The fullerenol nanoparticles size distribution in aqueous solutions of different concentrations and the electrokinetic potential measurements were carried out by dynamic light scattering on the Malvern Zetasizer (Great Britain) device. The relative uncertainty of the zeta-potential determination is equal to 5% ($\Delta\varsigma = \pm$ 5 arbitrary %).

Results and Discussion

Temperature Dependence of the Fullerenol Solubility in Water. The experimental data on densities of the fullerenol solutions is presented Figure 2a. The density of the fullerenol saturated solution increases monotonously with increasing of temperature, the shape of the temperature dependence of density is rather complex, the sigmoid curve was obtained (Figure 2a). Such type of dependence is influenced by the following factors:

- decreasing of water density and the fullerenol density in any aggregative state (there are no literature data on the fullerenol density, nevertheless the fact of the negative value of the $\partial\rho_{fullerenole}/\partial T$ derivative is also practically assured)
- increasing of the solubility values of the more dense fullerenol in the less dense water in the scale of mass concentrations of the saturated solutions
- weakening of the physical, in particular van der Waals forces and simultaneous increasing of the chemical interactions between solvent and solute molecules. Thus, the complex type of the temperature dependence of density is no marvel.

Figure 2b illustrates the monotonous increasing of the fullerenol solubility with increasing of temperature; the shape of the $S(T)$ curve is sigmoid.

Such form of the temperature dependence of solubility in the field of crystallization of the individual fullerene (or solid solvated fullerene) is not unusual. For example the temperature dependences of solubility in binary C_{70} + *o*-xylene system or the fields of crystallization of the sesqui-solvated fullerenes in C_{60} + α-cloronaphthalene and C_{60} + α-bromonaphthalene systems are characterized by sigmoid shape of the polytherms of solubility.[6,25−28,33]

Finally, we can state that the fullerenol solubility is extremely high for the light fullerenes and the light fullerenes derivatives. Practically similar values in the mass concentration and mass fraction scales correspond to solubility of such well-soluble salt as sodium chlorite. Moreover, the fullerenol solubility in water increases greatly with increasing of temperature higher than 50 °C and exceeds the sodium chloride solubility in the same concentration scales.

Partial Molar Volumes Calculation. The densities data of the fullerenol water solutions reveal that in the mass fraction range (0 to 0.0023) arbitrary units the extreme changing of density takes place.

Using the experimental data on densities the dependence between the fullerenol (1) partial molar volume V_1 and the fullerenol mole fraction (x_1) in solution was obtained (see Figure 3a).

$$\bar{V} = V/\sum_{i=1}^{2} n_i \qquad (2)$$

where V and n_i are the total volume and the j component number of moles.

The complex behavior of the $V_1(x_1)$ function in the area of low concentrations takes place. The $V_1(x_1)$ curve reaches a minimum at $x_1 \approx 0.00015$. This fact testifies of the structural compacting of solution with addition of negligible quantities of the fullerenol. On the contrary with increasing of the fullerenol concentration this effect disappears and the molar volume of the fullerenol solution increases.

To determine the obtained regularity we have calculated the fullerenol mole fraction dependences of the partial volumes of the components (V_1,V_2) at 25 °C (Figure 3, panels b and c). The partial volumes can be expressed as a following partial derivatives[20,30]

$$V_2 \equiv \left(\frac{\partial V}{\partial n_2}\right)_{T,P}, \quad V_1 \equiv \left(\frac{\partial V}{\partial n_1}\right)_{T,P} \qquad (3)$$

For the partial volumes calculation we have used the dependence between the partial and average molar functions:[30]

$$V_2 = \bar{V} - x_1\left(\frac{\partial \bar{V}}{\partial x_1}\right)_{T,P}, \quad V_1 = \bar{V} - x_2\left(\frac{\partial \bar{V}}{\partial x_2}\right)_{T,P} \qquad (4)$$

The partial derivatives $(\partial\bar{V}/\partial x_1)_{T,P}$ were calculated using a numerical approach.

Figure 3b shows the monotonous decreasing of the $V_2(x_1)$ function, the highest rate of decreasing take place in the area of low concentrations of the fullerenol ($x_1 \leq 0.000037$). Thus the compacting and structuring of the water molecules in solution takes place at low concentrations of the fullerenol. After that the $V_2(x_1)$ changing rate extremely decreases. Figure 3c shows the fast increasing of the $V_1(x_1)$ function in the area of low concentrations $x_1 \leq 0.000037$ to 0.000074. The high absolute values of the fullerenol partial molar volumes in the concentration range $x_1 < 0.000074$ are surprising. For example the fullerenol partial molar volume at $x_1 < 0.000074$ is equal to ≈ -10000 $cm^3 \cdot mol^{-1}$, in comparison the monomer fullerenes and the fullerene derivatives average molar volumes values are equal to 100 to 1000 $cm^3 \cdot mol^{-1}$. With the further increasing of the fullerenol concentration the V_1 value becomes positive

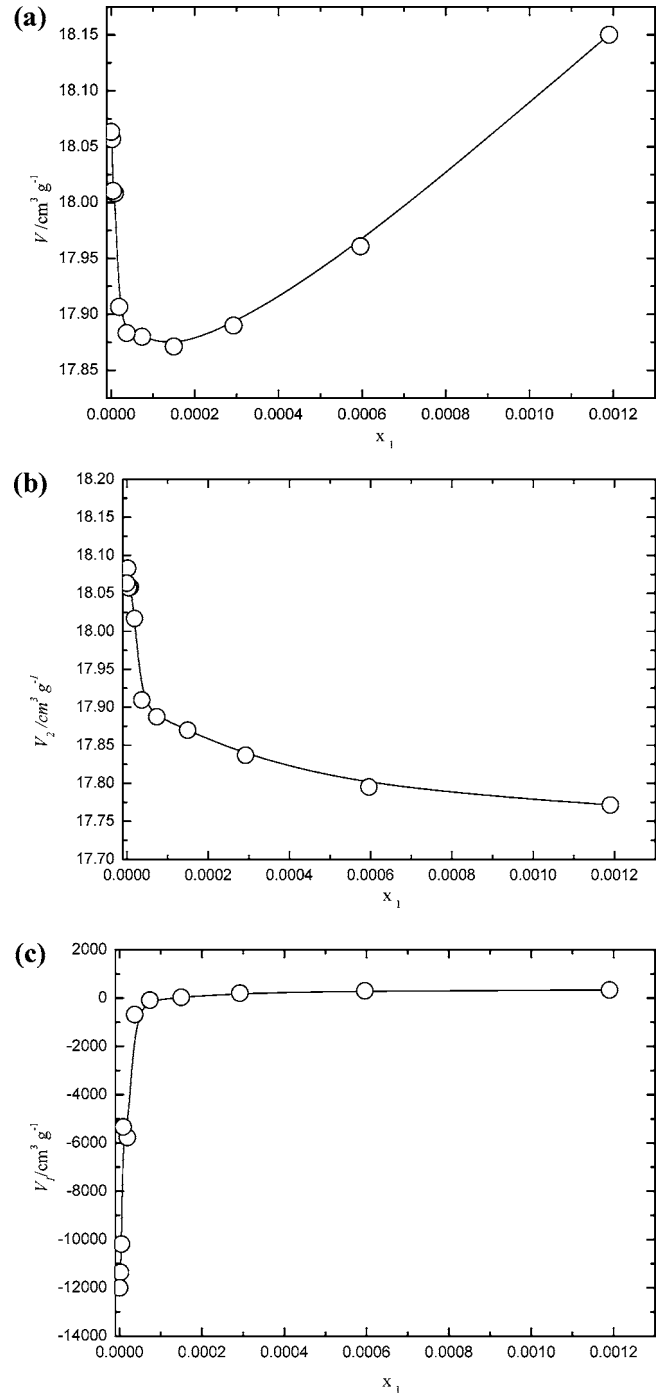

Figure 3. Mole fraction dependence of the average specific volume of the fullerenol + H_2O solutions (a) and mole fraction dependence of the partial volumes of the solutions components (b and c) at 25 °C. V_1 - specific volume of the fullerenol, V_2 - specific volume of water, x_1 - the fullerenol mole fraction in solution.

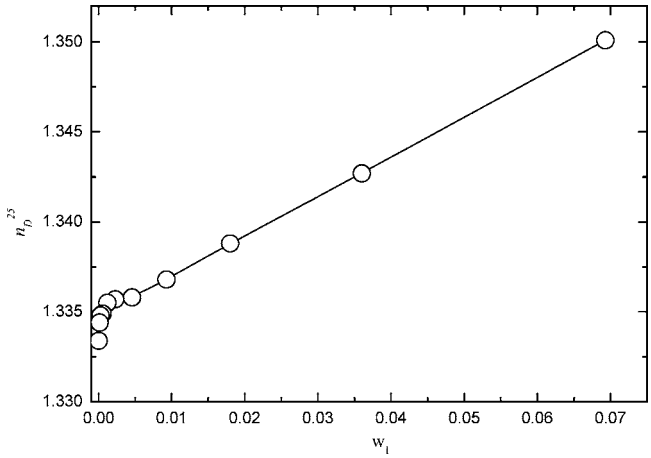

Figure 4. Mass fraction dependence of the refraction index (n_D^{25}) of the fullerenol water solutions. w_1 is the mass fraction of the fullerenol.

and close to the desired values. For example, the partial molar volume at $x_1 \approx 0.00119$ is equal to 340 $cm^3 \cdot mol^{-1}$. The latest fact demonstrates that the fullerenol molecules are naturally embedded to the structure of solution and occupy the volume corresponding to electronic structure.

Mass Fraction Dependence of the Refraction Index. The experimental data on refractive indexes of the fullerenol water solutions are presented in Figure 4. Analogous case of sharp increasing of the $n_D^{25}(w_1)$ function in the area of highly diluted solutions (up to the 0 to 0.0023 values of mass fraction) takes place. After further increasing of the fullerenol concentration the rate of the n_D^{25} function change is stable and the dependence between the refractive index and mass fraction of the fullerenol becomes linear. The similar dependences take place in the case of specific refraction (r) of water fullerenol solutions[31]

$$r = \left(\frac{n_D^{25^2} - 1}{n_D^{25^2} + 2}\right)\frac{1}{\rho} \qquad (5)$$

where ρ is the solution density.

The decreasing of the specific refraction with increasing of the fullerenol mass fraction (in the area of highly diluted solutions $w_1 \leq 0.0023$ was observed; after that the dependence becomes linear. This fact indirectly testifies that in the process of addition of negligible quantities of fullerenol the changing of the solution components electronic structure takes place. The further increasing of the fullerenol concentration leads to leveling of this effect.

Molarity Dependence of the Hydrogen Ion Concentration and Hydroxyl-Ion Concentration of the Fullerenole Water Solution. The dependences between the hydrogen ion concentration (pH) as well as hydroxyl-ion concentration of the fullerenol water solutions and the molar concentration of the fullerenol are presented on Figure 5, panels a and b.

The analysis of the presented plots shows, that the fullerenol solutions have the alkaline medium. In other words the alkaline (acidic) dissociation mechanism according to reaction

$$C_{60}(OH)_{22\div24} \rightarrow [C_{60}(OH)_{21\div23}O]^- + H^+ \qquad (6)$$

cannot be realized. Thus, the name of fullerenol (with the alkaline index "-ol") is not correct for the fullerenol obtained

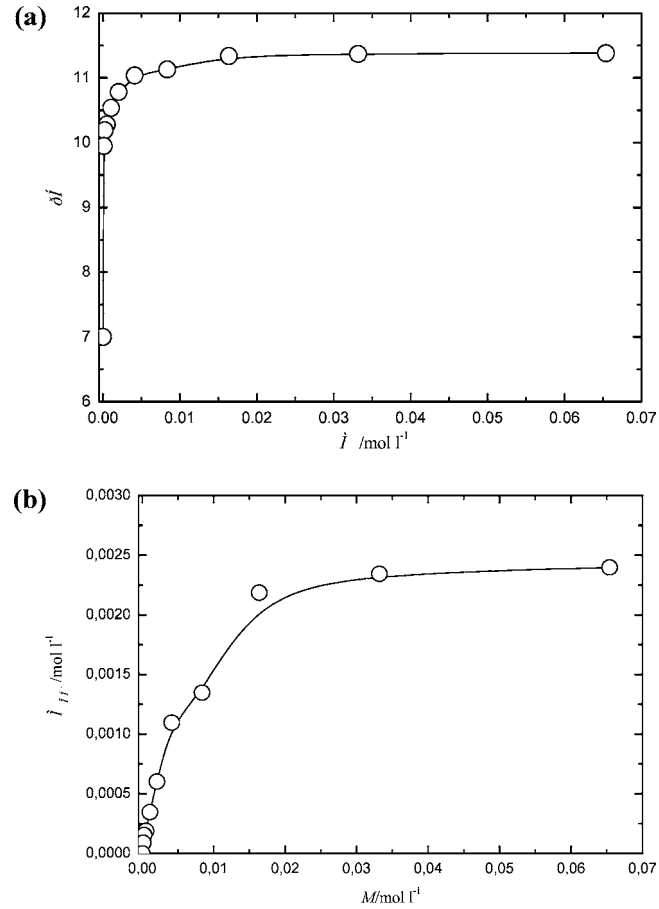

Figure 5. Molarity dependence (M) of the hydrogen ion concentration (a) and the hydroxyl ion concentration (b) of the fullerenol water solution at 25 °C. M is the molarity of the fullerenol solution.

by the described in this paper method, in spite of this the name of compound is generally accepted.

Another dissociation mechanism explaining the observed effect can be expressed by the following reaction:

$$C_{60}(OH)_{22\div24} \rightarrow [C_{60}(OH)_{21\div23}]^+ + OH^- \qquad (7)$$

It is noteworthy that even highly diluted fullerenol solutions (at $c_1 \approx 0.00013$ mol·L^{-1}) among investigated are violently alkalinize the water solution. The hydrogen ion concentration value at $c_1 \approx 0.00013$ mol·L^{-1} is equal to 9.95 arbitrary units. The further rate of hydrogen ion concentration increasing with increasing of the fullerenol concentration decreases and becomes stable.

The dependence between the fullerenol apparent degree of dissociation and molarity of solution is presented in Figure 6a. The valuating calculation of the degree of dissociation was performed at the following simplification:

- the hydroxide ions excess thermodynamic functions (activity coefficients) were not taken into account. Thus the hydroxide ion activity coefficient is equal to the hydroxide ion molarity ($a_{OH^-} \approx M_{OH^-}$)
- only the first stage of the fullerenol dissociation can be carried, the further stages (eq 8)

cannot be realized

$$[C_{60}(OH)_{22-n\div24-n}]^{n+} \rightarrow [C_{60}(OH)_{22-n-1\div24-n-1}]^{(n+1)+} + OH^- \quad (8)$$

Thus the fullerenol degree of dissociation can be expressed by the following equation:

$$\alpha_{\text{fullerenole}} \approx \frac{M_{OH^-}}{M_{\text{fullerenol}}} \quad (9)$$

The calculation carried under above-mentioned assumptions allows to conclude that in the concentration range 0.001 mol·L^{-1} $\leq C_{\text{fullerenol}} \leq$ 0.07 mol·L^{-1} the fullerenol is a medium electrolyte and when the concentrations lower than 0.001 mol·L^{-1} the fullerenol is a moderately strong electrolyte.

The dependence between the negative common logarithm of the concentration dissociation constant and molarity of solution ($pK = -\log[K_d(c_1)]$) is presented in Figure 6b. The valuating calculation of the dissociation constant was performed under the same simplifying assumptions used for the degree of dissociation determination. Additionally the undissociated fullerenol and fullerenol ion excess thermodynamic functions (activity coefficients) were neglected.

Concentration Dependence of Specific Conductivity of the Fullerenole Water Solutions. Determination of the Fullerenol Chemical Formula. The experimental data on mass fraction dependence of the specific conductivity (σ) of the fullerenol water solutions show that the monotonous increasing of the specific conductivity with increasing of concentration takes place. The $\sigma_{(\text{wfullerenol})}$ curve does not riches maximum values typical for strong electrolytes.[29] The molar conductivity was calculated according to formula (10):

$$\lambda = 1000\sigma/M_{\text{fullerenol}} \quad (10)$$

The analysis of the obtained dependence shows the decreasing of the molar conductivity values with increasing of the fullerenol mole fraction. The limiting value of molar conductivity $\lambda_0 = \lambda(M_{\text{fullerenol}} \rightarrow 0) \approx 200$ S cm^2·mol^{-1} is well agreed with the corresponding value of λ_0 for the hydroxyl ion.[22] This fact indicates, that the $[C_{60}(OH)_{21\div23}]^+$ fullerenol-ions practically does not participate in the process of charge transfer, in other words the fullerenol ion transfer numbers are not significant ($t_{[C_{60}(OH)_{21\div23}]^+} \approx 0$, $t_{OH^-} \approx 1$).

The λ_0 value was obtained by the linear extrapolation of the $\lambda = \lambda(\sqrt{M_{\text{fullerenol}}})$ dependence.[34]

On the basis of molar conductivity data the concentration dependence of the fullerenol apparent degree of dissociation was calculated (Figure 6a)

$$\alpha = \lambda/\lambda_0 \quad (11)$$

If we assume that the one-stage dissociation process of fullerenol takes place, the fullerenol can be represented as a strong electrolyte in the investigated molarity range ($M \leq$ 0.0654 mol·L^{-1}), the apparent degree of dissociation is equal to $\alpha \geq$ 0.35.

We can also assume that the main charge carrier particle is a hydroxyl ion in one's turn we can neglect by the process of charge transferring of "heavy" fullerenol ions.

It was determined that at low concentrations of fullerenol ($M \leq$ 0.0003 mol·L^{-1}) the apparent degrees of dissociation (α) calculated from the data on conductivity and from pH data are close. On the contrary, at comparatively high concentrations of fullerenol ($M \geq$ 0.03 mol·L^{-1}) the difference increases and reaches order. We suppose, that this fact can be explained by the following reasons:

- For the apparent degrees of dissociation calculations we have admitted an assumption that the hydroxyl ion activity coefficient (in the molarities scale) in the fullerenol solution is equal to 1 ($\ln \gamma_{OH^-} = 0$). Apparently, the activity coefficient value is less than 1, and consequently the real molarity of the hydroxyl ion in solution is higher than molar activity. Naturally such inaccuracy increases with increasing of concentration. The latest fact well agreed with Figure 6a.

We have assumed that the conditions of charge transferring in the "infinitely diluted solution" of fullerenol and in "finitely diluted solution" are close. The difference between λ and λ_0 values are connected with dissociation process (nondissociated fullerenol molecules are nonconductive). If we assume that in rather diluted solutions ($M \approx$ 0.0003 mol·L^{-1}) the conductive structural network, which help to transfer the charge was formed the increasing of measured values of molar conductivity (and the degree of dissociation calculated values) can be explained. At high dilutions (M = 0.0003 → 0 mol·L^{-1}) this effect is negligible. The dependence between the negative common logarithm of the fullerenol dissociation constant (pK) and molarity of the fullerenol solution is presented in Figure 6b.

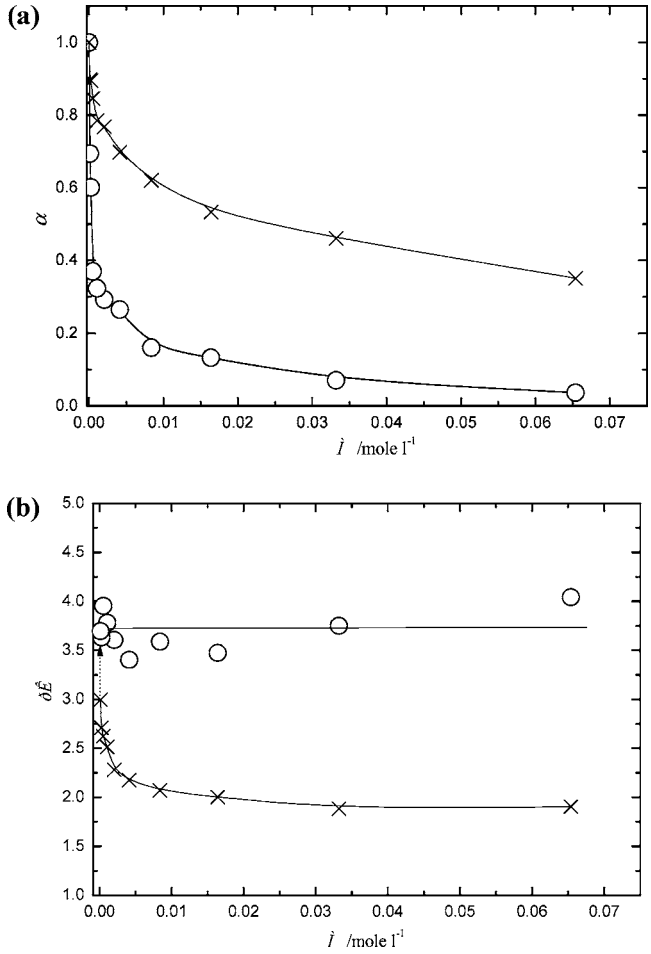

Figure 6. Molar concentration dependences of the apparent degree of dissociation (a) and the concentration dissociation constant (b) in the fullerenol water solution at 25 °C. ×, from the electroconductivity data; ○, from the hydrogen ion concentration data.

The fullerenol dissociation constant calculation was carried out on the basis of electroconductivity data using the Ostwald equation.

In this case at low concentrations of fullerenol ($M \leq 0.0003$ mol·L^{-1}), the concentration dissociation constants, K_d, calculated from the pH and electroconductivity data are close. On the contrary at relatively high concentrations ($M \geq 0.03$ mol·L^{-1}), the difference between dissociation constants increases and reaches two orders. The dissociation constant (K_d) limiting values in the infinitely diluted solutions correspond to the first stage thermodynamic dissociation constant ($K_d \approx 3.6 \pm 0.3$).

The experimental data on titration of the fullerenol water solutions by H_2SO_4 solution reveals the presence of two effects corresponding to the following titration volumes of sulphuric acid 6 and 41 mL. These volumes correspond to $2.40 \cdot 10^{-5}$ and $1.64 \cdot 10^{-4}$ mol of H_2SO_4 and $4.80 \cdot 10^{-5}$ and $3.28 \cdot 10^{-4}$ gram-ions of H^+.

Thus the first titration effect corresponds to interaction of at least two ions H^+/1 mol of fullerenol [$n_{\text{fullerenol}}/n_1(H^+)$] $\approx$ 1/2, the second titration effect corresponds to interaction of fourteen ions H^+/1 mol of fullerenol [$n_{\text{fullerenol}}/n_1(H^+)$] $\approx$ 14.

Let us assume that $[C_{60}(OH)_{n1}O_{n2}](ONa)_{n3}$ is the general formula of fullerenol and make several propositions:

- not half of hydroxyl-ions are equivalent in the fullerenol molecule
- non-hydrogenized oxo-groups O_{n_2} are inert in the acid−base meaning
- sodium-substituted groups $(ONa)_{n_3}$ first of all react with ions H^+ according to reaction

$$[C_{60}(OH)_{n_1}O_{n_2}](ONa)_{n_3} + n_3/2H_2SO_4 \rightarrow [C_{60}(OH)_{n_1+n_3}O_{n_2}] + n_3/2Na_2SO_4 \quad (12)$$

- then in the acid region the reaction between the hydroxyl ions of the fullerenol molecule and H_2SO_4 begins. The process of substitution of hydroxyl ions by sulphates groups performs according to reaction

$$[C_{60}(OH)_{n_1+n_3}O_{n_2}] + (\Delta n)/2H_2SO_4 \rightarrow [C_{60}(OH)_{n_1+n_3-\Delta n}(SO_4)_{\Delta n/2}O_{n_2}] + \Delta n/2Na_2SO_4 \quad (13)$$

- we consider that not half of hydroxyl groups in the fullerenol molecule are titrated by H_2SO_4 at pH $\geq$ 3, some of them are "free". The fact of inequality of hydroxyl groups is not surprising, due to in the process of the fullerenol synthesis OH groups can be associated with hexagonal and pentagonal carbon atoms of the fullerene molecule.

Then

- from the first effect of the potentiometric titration follows that in average $n_3 \approx 2$, this fact is marginally corroborated by the qualitative results of mass-spectrometric investigation
- from the second effect of the potentiometric titration follows that in average $\Delta n \approx 14$
- from the qualitative results obtained from the mass-spectrometric investigation we have revealed the typical value of $n_2 = 0 \div 3$. Hereinafter we assume that in average $n_2 \approx 2$

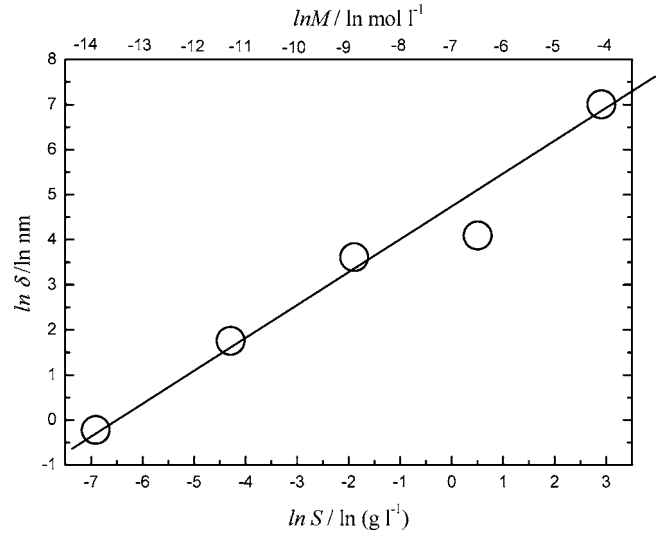

Figure 7. Average size of the fullerenol associates in the fullerenol water solutions in the logarithmic scale.

- on the basis of mass-spectrometric study we have determined the average total number of oxygen atoms in the fullerenol molecule, consequently $n_1 + n_2 + n_3 \approx 22 \div 24$
- from the $18 \div 20$ residuary hydroxyl groups $(OH)_{18\div20}$ about 14 can be titrated by sulphuric acid at pH $\geq$ 3 (active hydroxyl groups $(OH)^{act}$) and about $4 \div 6$ in this conditions remain free (inactive groups $(OH)^{inact}$)

Thus, we suppose that the most probable averaged formula of fullerenol is $[C_{60}(OH)_{18\div20}O_{0\div3}](ONa)_{2\pm1}$ or more exactly $[C_{60}(OH)^{act}_{14\pm1}(OH)^{inact}_{4\div6}O_{0\div3}](ONa)_{2\pm1}$.

The experimental data on titration of the fullerenol water solutions by NaOH solution show the presence of a single effect, corresponding to titration volume of NaOH solution equal to 0.1 mL. This volume corresponds to $1.00 \cdot 10^{-3}$ mol of NaOH and $1.00 \cdot 10^{-3}$ gram-ions of OH^-. Thus the single titration effect corresponds to interaction in average of 5 OH^--ions$^-$/ 1 mol of fullerenol [$n_{\text{fullerenole}}/n_1(OH^-)$] $\approx$ 1/5 arbitrary units. Obviously at pH $\approx$ 11.4 the titration of "relatively acid and inactive" hydroxyl groups takes place. These groups become active under conditions of alkaline titration.

Consequently the following process takes place for the fullerenol molecules

$$[C_{60}(OH)^{act}_{14\pm1}(OH)^{inact}_{4\div6}O_{0\div3}](ONa)_{2\pm1} + 5NaOH \rightarrow [C_{60}(OH)^{act}_{14\pm1}O_{0\div3}](ONa)_{7\pm1} + 5H_2O$$

This process marginally corroborates the determined in the previous section formula of the fullerenol.

Associate Size Distribution in the Fullerenol Water Solutions. Zeta-Potential Measurements. The typical dependence of the associate size distribution in the fullerenol water solutions is presented in Figure 7 and Table 1. The fullerenol concentration was varied in a wide range from 0.0137 g·L^{-1} up to 18.3 g·L^{-1} ($M_{\text{fullerenol}} \approx 1.2 \cdot 10^{-5} \div 1.5 \cdot 10^{-2}$ mol·L^{-1}). Unfortunately, more concentrated fullerenol solutions (in particular $M_{\text{fullerenol}} \approx 0.17$ mol·L^{-1}) are opaque and the method of associate size determination used is unserviceable.

Analysis of Figure 7 shows the following:

- With increasing of the fullerenol concentration, the associate average diameter increases. With increasing of the

Table 1. Average Size of the Fullerenol Associates and the Average Number of the Fullerenol Molecules in Water Solutions[a]

	S	*M*	δ	
no.	$g \cdot L^{-1}$	$mol \cdot L^{-1}$	nm	*N*
1[b]	0	0	1.8	$\approx 1 \cdot 10^0$
2	0.0137	0.000012	5.8	$\approx 2 \cdot 10^1$
3	0.151	0.00013	37	$\approx 4 \cdot 10^3$
4	1.66	0.0014	60	$\approx 2 \cdot 10^4$
5	18.3	0.015	1100	$\approx 2 \cdot 10^7$
6	201	0.17	opaque solution	opaque solution

[a] *S*, volume concentration of fullerenol, *M*, molar concentration of the fullerenol solution, δ, average diameter of the fullerenol associate, and *N*, number of the fullerenol molecules in the fullerenol associate. [b] The data were obtained by direct calculation.

fullerenol concentration from 1.66 $g \cdot L^{-1}$ to 18.3 $g \cdot L^{-1}$ (samples nos. 4 and 5) the most impetuous growing of the fullerenol associate size take place ($\delta \approx 60 \rightarrow 1100$ nm).

- The fullerenol associates size distribution is rather "sharp" (especially taking into account the complex composition of their mixture). Thus, the intensity peak half-width ($\delta_{1/2}$) is equal to 1 arb. units. This value corresponds to no more than one order difference in the associate sizes.
- No nonassociated fullerenol particles (with diameter $\delta <$ 2 nm) were detected by dynamic light scattering in the sample series nos. 2−5. Consequently, even highly diluted solutions are strongly associated.
- Analysis of the dependence between the average size of the fullerenol associates and concentration of the fullerenol solution in logarithmic scale shows, that the stable linear correlation between these functions in logarithmic form takes place. In other words the $\delta(C_{\text{fullerenol}})$ dependence can be represented by the following expression: $\delta = \alpha C_{\text{fullerenol}}^{\beta} + \delta_0$, where α and β are constants and δ_0 is a calculated diameter of a monomeric hydrated fullerenol molecule at $C_{\text{fullerenol}} \rightarrow 0$. Obviously, in all cases $\delta_0 \ll \delta(C_{\text{fullerenol}} \neq 0)$.

Let us dwell on the evaluative calculation of δ_0. From general considerations follows that

$$\delta_0 \approx \delta(C_{60}) + 2[r(C - O) + r(O - H) + \delta(H_2O) + r(O\cdots H)] \quad (14)$$

where $\delta(C_{60}) \approx 0.68$ nm, according to ref 1, "diameter" of the C_{60} molecule, $r(C-O) \approx 0.14$ nm is a C−O bond distance of the aliphatic alcohols,[32] $r(O-H) \approx 0.10$ nm is a O−H bond distance,[34] $\delta(H_2O) \approx 0.14$ nm "diameter" of the H_2O molecule in the spheroidal approximation (this value was calculated from the polarizability of the water molecule $\alpha(H_2O) \approx 1/6\pi\delta(H_2O)^3$),[34] $r(O\cdots H) \approx 0.20$ nm is a O···H hydrogen bond distance.[35]

As a result, the evaluative value of $\delta_0 \approx 1.8$ nm (see Table 1) was determined.

The dependence between the average number of the fullerenol monomeric particles in one associate and the fullerenol concentration (*N*) in water solution in logarithmic scale is presented in Figure 7. The calculation was carried out according to formula 15

$$N = \left[\frac{\delta}{\delta_0}\right]^3 [K_{\text{packing}}^{\text{spheroid}}]^W \quad (15)$$

where $K_{\text{packing}}^{\text{spheroid}}$ is a formal packing coefficient (ratio of volume occupied by monomeric fullerenol molecules in the associate to the total volume of associate. The packing coefficient equal to $K_{\text{packing}}^{\text{spheroid}} = 1/2$ arbitrary units was taken up for the evaluation. This value is practically the same as the $K_{\text{packing}}^{\text{spheroid}}$ value for the pure water and slightly less than in the case of close packing by spheroids ($K_{\text{packing}}^{\text{spheroid}}(\text{max}) \approx 0.74$ arbitrary units). *W* is a fullerenol associate or "percolation cluster" order. Actually the fullerenol monomeric molecules can be packed by two basically different ways (Figure 8). The variant of the "percolation clusters" equilibration with each other and with monomeric molecules is presented in Figure 8(left).[36] The multilevel structure, when the primary percolation cluster is formed by monomeric molecules, the secondary cluster is formed by the primary percolation clusters, the tertiary cluster-by the secondary percolation clusters is presented in Figure 8 (right). The authors

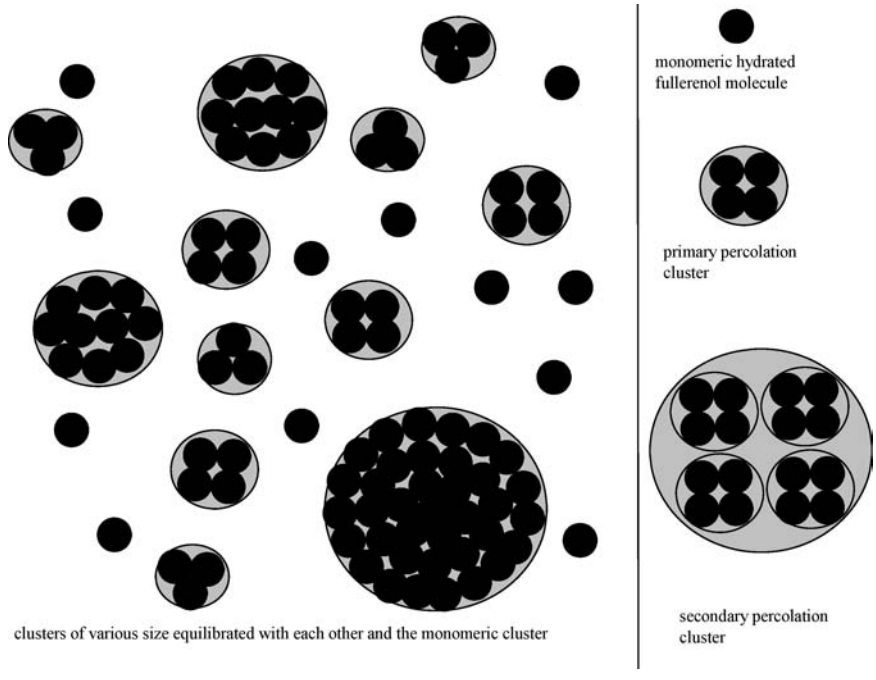

Figure 8. Types of the fullerenol clusters association.

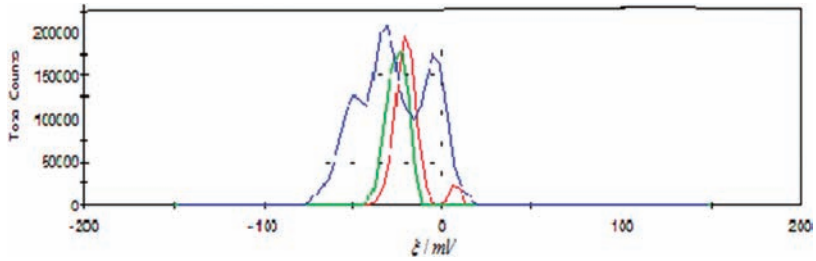

Figure 9. ζ-potential dependence of number of the registered signals (reflexes situated from left to right correspond to solutions 4, 3, and 2 from Table 1).

presume the second type of the cluster organization in the fullerenol solution due to the clusters of various size equilibrated with each other and the monomeric clusters were not observed in the fullerenol solution.

- In our case for the fullerenol monomer $W = 0$ (solution N1), for the fullerenol associates in solutions $N = 2 \div 4$ and $W = 1$ and 2, for the fullerenol associates in solutions $N = 5$ and $W = 3$ (see Table 1).
- At the 18.3 $g \cdot L^{-1}$ fullerenol concentration, the number of particles is equal to 2×10^7. This fact corresponds to destroying of the liquid solution homogeneity and forming of a microcolloid solution.

It is known that in the process of the dispersion phase relative displacement the discontinuity of the double electrical layer formed in the sliding boundary takes place. Due to the sliding plane pass through the diffuse layer and part of ions are in the dispersion phase the disperse medium and the dispersion phase are conversely charged. The potential originated in the sliding plane in the part of the diffuse layer separation process is a ζ-potential.[37−40]

The dependence between the number of the registered signals (R) and zeta-potential is presented in Figure 9 (the reflexes disposed from left to right correspond to solutions with numbers 4, 3, and 2 (see Table 1)).

Due to opacity of the solution no. 6 the zeta-potential measurements are noninformative. Owing to extremely low concentration of the gigantic associates the investigation of the solution no. 5 cannot be carried. The molar concentration of the monomeric fullerenol in the solution no. 5 is equal to 0.016 $mol \cdot L^{-1}$ in one's turn the molarity of the fullerenol associates is equal to 8×10^{-10} $mol \cdot L^{-1}$. Such low concentration cannot give any reflexes by the dynamic light scattering. Figure 9 also shows that for rather diluted solutions only the one reflex is presented on the $R(\zeta)$-dependence, in the case of more concentrated solution ($C_{fullerenol} \approx 1.66$ $g \cdot L^{-1}$) the $R(\zeta)$-dependence includes 3 reflexes. The latest fact indirectly confirms the fact of complex organization of the fullerenol percolation clusters in rather concentrated solutions.

Conclusions

The fullerenol identification was carried out by the methods of IR spectroscopy, UV spectroscopy, optical microscopy, and mass-spectrometry. The concentration dependence of density was investigated by the picnometer method; the average molar and partial volumes of the solution components were calculated at 25 °C. The concentration dependence of the refractive index was investigated by the refractometric method. By the isothermal saturation method the fullerenol solubility in the distilled water in the temperature range 20 to 80 °C was studied. On the basis of the pH-potentiometric method, the data on concentration dependence of the hydrogen ion concentration was obtained; the dissociation constant as well as the apparent degree of dissociation were calculated. The specific conductivity, molar conductivity, dissociation constant, and the apparent degree of dissociation were obtained for the fullerenol water solutions. By the dynamic light scattering method, the average size of the fullerenol associates and the concentration dependence of the ζ-potential were determined.

Supporting Information Available:

IR spectrum and mass-spectrum of the fullerenol, derivatogram of the fullerenol crystallohydrate, mass fraction dependence of the specific refraction, mass fraction and mole fraction dependences of the specific and molar electroconductivities, integral and differential plots of the potentiometric titration of the fullerenole water solutions, and polarizing microscope photos of the fullerenole crystals. This material is available free of charge via the Internet at http://pubs.acs.org.

Literature Cited

(1) Sidorov, L. N.; Yurovskaya, M. A. *Fullerenes*; Ekzamen: Moscow, 2005.
(2) Semenov, K. N.; Arapov, O. V.; Charykov, N. A. The solubility of fullerenes in *n*-alkanols-1. *Russ. J. Phys. Chem.* **2008**, *82*, 1318–1326.
(3) Heyman, D. Solubility of C_{60} in alcohols and alkanes. *Carbon.* **1996**, *34*, 627–631.
(4) Beck, M. T.; Mandi, G. Solubility of C_{60}. *Fullerene Sci. Technol.* **1997**, *5*, 291–310.
(5) Korobov, M. V.; Smith, A. L. Solubility of Fullerenes. In *Physics and Technology*; Kadish, K. M., Ruoff, R. S., Eds.; John Wiely & Sons: New York, 2000; pp 53−59.
(6) Semenov, K. N.; Charykov, N. A.; Keskinov, V. A.; Piartman, A. K.; Blokhin, A. A.; Kopyrin, A. A. Solubility of light fullerenes in organic solvents. *J. Chem. Eng. Data* **2009**, *55*, 13–36.
(7) Heymann, D. Solubility of Fullerenes C_{60} and C_{70} in Seven Normal Alcohols and Their Deduced Solubility in Water. *Fullerene Sci. Technol.* **1996**, *4*, 509–515.
(8) Heymann, D. Solubility of fullerenes C_{60} and C_{70} in water. *Lunar Planetary Sci.* **1996**, *27*, 543–544.
(9) Semenov K. N.; Charykov, N. A.; Keskinov, V. A.; Pyartman, A. K.; Arapov, O. V. *Russ. J. Appl. Chem.* **2010**, ASAP.
(10) Li, J.; Takeuchi, A.; Ozawa, M.; Li, X.; Saigo, K.; Kitazawa, K. C_{60} fullerole formation catalyzed by quaternary ammonium hydroxide. *J. Chem. Soc. Chem. Commun.* **1993**, *22*, 1784–1785.
(11) Chiang, L. Y.; Bhonsle, J. B.; Wang, L.; Shu, S. R.; Chang, T. M.; Hwu, R. J. Efficient one-flask synthesis of water-soluble [60] fullerenols. *Tetrahedron* **1996**, *52*, 4963–4672.
(12) Chiang, L. Y.; Upasani, R. B.; Swirczewski, J. W. Versatile nitronium chemistry for C_{60} fullerene functionalization. *J. Am. Chem. Soc.* **1992**, *114*, 10154–10157.
(13) Meier, M. S.; Kiegiel, J. Preparation and characterization of the fullerene diols 1,2-$C_{60}(OH)_2$, 1,2-$C_{70}(OH)_2$, and 5,6-$C_{70}(OH)_2$. *Org. Lett.* **2001**, *3*, 1717–1719.
(14) Szymanska, L.; Radecka, H.; Radecki, J.; Kikut-Ligaj, D. Fullerene modified supported lipid membrane as sensitive element of sensor for odorants. *Biosens. Bioelectron.* **2001**, *16*, 911–915.
(15) Mirkov, S. M.; Djordjevic., A. N.; Andric, N. L.; Andric, S. A.; Kostic, T. S.; Bogdanovic, G. M.; Vojinovic-Miloradov, M. B.; Kovacevic, R. Z. Nitric oxidescavenging activity of polyhydroxylated fullerenol, $C_{60}OH_{24}$. *Nitric Oxide* **2004**, *11*, 201–207.
(16) Kokubo, K.; Matsubayashi, K.; Tategaki, H.; Takada, H.; Oshima, T. *ACS Nano* **2008**, *2*, 327–333.
(17) Yang, J. M.; He, W.; Ping, W. *Chin. J. Chem.* **2004**, *22*, 1008–1011.

(18) Sheng, W.; Ping, H.; Jian-Min, Z.; Hu, J.; Shi-Zheng, Z. *Synth. Commun.* **2005**, *35*, 1803–1808.
(19) Long, Y. United States Patent 5,648,523. Chiang, July 15, 1997.
(20) Semenov, K. N.; Charykov, N. A.; Letenko, D. G.; Nikitin, V. A.; Postnov, V. N.; Krokhina, O. A. Synthesis and identification of fullerenol. *Vestnik of Saint-Petersburg State University* 2010, ASAP.
(21) Piotrovskij, L. B.; Kiselev, O. I. *Fullerenes in biology*; Rostok: Saint-Petersburg, 2006.
(22) Pinteala, M.; Dascalu, A.; Ungurenasu, C. Binding fullerenol $C_{60}(OH)_{24}$ to dsDNA. *Int. J. Nanomed.* **2009**, *4*, 193–199.
(23) Semenov, K. N.; Charykov, N. A.; Namazbaev, V. I.; Arapov, O. V.; Pavlovetz, V. V.; Keskinov, V. A.; Pjartman, A. K. Solubility of light fullerenes in natural oils. *Russ. J. Gen. Chem.* **2009**, *79*, 1323–1330.
(24) Semenov, K. N.; Charykov, N. A.; Arapov, O. V. Temperature dependence of solubility of light fullerenes in natural oils and animal fats. *Fullerenes, Nanotubes Carbon Nanostruct.* **2009**, *17*, 230–248.
(25) Sivarman, N.; Dhamodaran, R.; Kallippan, I.; Srinivassan, T. G.; Vasudeva, P. R.; Mathews, C. K. Solubility of C_{60} in organic solvents. *J. Org. Chem.* **1992**, *57*, 6077–6079.
(26) Chen, W.; Xu, Z. Temperature dependence of C_{60} solubility in different solvents. *Fullerene Sci. Technol.* **1998**, *6*, 285–290.
(27) Doome, R. J.; Dermaut, S.; Fonseca, A.; Hammida, M.; Nagy, J. B. New evidence for the anomalous temperature-dependent solubility of C_{60} and C_{70} fullerenes in various solvents. *Fullerene Sci. Technol.* **1997**, *5*, 1593–1606.
(28) Tian, J. Comparative solubility study of C_{60} and C_{60}-piperazine and applications on quartz crystal microbalance/heat conduction calorimeter. A Thesis Submitted to the Faculty of Drexel University by Jun Tian in partial fulfillment of the requirements for the degree of Doctor of Philosophy, 2002.
(29) Mischenko, K. P.; Ravdel, A. A.; Ponomareva, A. M. *Practical works on physical chemistry*; Khimia: Leningrad, 1982.
(30) Storonkin, A. V. *Thermodynamics of heterogeneous systems*; Leningrad State University: Leningrag, 1967.
(31) Ioffe, B. V. *Refractometric methods*; Khimia: Leningrad, 1983.
(32) Mischenko, K. P.; Ravdel', A. A. *Abstract of physical-chemical properties*; Khimija: Leningrad, 1974.
(33) Semenov, K. N.; Charykov, N. A. Temperature dependence of solubility of individual light fullerenes and industrial fullerene mixture in 1-chloronaphthalene and 1-bromonaphthalene. *J. Chem. Eng. Data* **2010**, in press.
(34) Pentin, Yu. A.; Vilkov, L. V. *Physical methods in chemistry*; Mir: Moscow, 2003.
(35) Emsley, J. Very Strong Hydrogen Bonds. *Chem. Soc. Rev.* **1980**, *9*, 91–124.
(36) Gelashvili, D. B.; Iudin, D. I. Fractal structure of percolation clusters and space distribution of the dominate types. *Dokladi Akademii Nauk.* **2006**, *4*, 560–563.
(37) Frolov, Yu. G. Colloid chemistry. *Surface phenomena and dispersions*; Khimia: Moscow, 1982.
(38) Internet resource http://www.metalinfo.ru/ru/directory/list.
(39) Stromberg, A. G. *Physical Chemistry*; Visshaja Shkola: Moscow, 1973.
(40) Damaskin, B. B.; Petrii, O. A. *Introduction to electrochemical kinetics*; Khimia: Moscow, 1983.

Received for review August 6, 2010. Accepted December 27, 2010. The work was supported by Russian Found of Fundamental Researches (Project No. 09-03-00350-a).

JE100755V